

UNCLASSIFIED

AD NUMBER

ADB004699

LIMITATION CHANGES

TO:

Approved for public release; distribution is unlimited.

FROM:

Distribution authorized to U.S. Gov't. agencies only; Test and Evaluation; MAY 1975. Other requests shall be referred to U.S. Army Ballistic Research Laboratories, Attn: AMXBR-SS, Aberdeen Proving Ground, MD 21005.

AUTHORITY

USAARDC ltr, Apr 1978

THIS PAGE IS UNCLASSIFIED

THIS REPORT HAS BEEN DELIMITED
AND CLEARED FOR PUBLIC RELEASE
UNDER DOD DIRECTIVE 5200.20 AND
NO RESTRICTIONS ARE IMPOSED UPON
ITS USE AND DISCLOSURE.

DISTRIBUTION STATEMENT A

APPROVED FOR PUBLIC RELEASE;
DISTRIBUTION UNLIMITED.

BRL R 1781

BRL

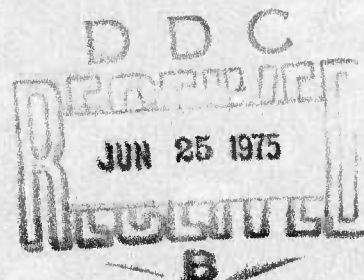
AD

ADB004699

REPORT NO. 1781

PROPAGATION CHARACTERISTICS OF NARROW X-RAY PULSES

Heber D. Jones
Donald Eccleshall
Judith K. Temperley



May 1975

Distribution limited to US Government agencies only; Test and Evaluation; MAY 75; Other requests for this document must be referred to Director, USA Ballistic Research Laboratories, ATTN: AMXBR-SS, Aberdeen Proving Ground, Maryland 21005.

USA BALLISTIC RESEARCH LABORATORIES
ABERDEEN PROVING GROUND, MARYLAND

Destroy this report when it is no longer needed.
Do not return it to the originator.

Secondary distribution of this report by originating
or sponsoring activity is prohibited.

Additional copies of this report may be obtained
from the Defense Documentation Center, Cameron
Station, Alexandria, Virginia 22314.

The findings in this report are not to be construed as
an official Department of the Army position, unless
so designated by other authorized documents.

UNCLASSIFIED

SECURITY CLASSIFICATION OF THIS PAGE (When Data Entered)

REPORT DOCUMENTATION PAGE		READ INSTRUCTIONS BEFORE COMPLETING FORM	
1. REPORT NUMBER REPORT NO. 1781	2. GOVT ACCESSION NO.	3. RECIPIENT'S CATALOG NUMBER	
4. TITLE (and Subtitle) Propagation Characteristics of Narrow X-Ray Pulses		5. TYPE OF REPORT & PERIOD COVERED 1 July 73 - 30 June 74	
		6. PERFORMING ORG. REPORT NUMBER	
7. AUTHOR(s) Heber D. Jones, Donald Eccleshall, and Judith K. Temperley		8. CONTRACT OR GRANT NUMBER(s)	
9. PERFORMING ORGANIZATION NAME AND ADDRESS USA Ballistics Research Laboratories Aberdeen Proving Ground, Maryland 21005		10. PROGRAM ELEMENT PROJECT, TASK AREA & WORK UNIT NUMBERS RDTC Project No. 1T161101A91A	
11. CONTROLLING OFFICE NAME AND ADDRESS US Army Materiel Command 5001 Eisenhower Avenue Alexandria, Virginia 22304		12. REPORT DATE MAY 1975	
		13. NUMBER OF PAGES 34	
14. MONITORING AGENCY NAME & ADDRESS (if different from Controlling Office)		15. SECURITY CLASS. (of this report) Unclassified	
		15a. DECLASSIFICATION/DOWNGRADING SCHEDULE	
16. DISTRIBUTION STATEMENT (of this Report) Distribution limited to US Government agencies only; Test and Evaluation; May 1975. Other requests for this document must be referred to Director, USA Ballistic Research Laboratories, ATTN: AMXBR-SS, Aberdeen Proving Ground, Maryland 21005			
17. DISTRIBUTION STATEMENT (of the abstract entered in Block 20, if different from Report)			
18. SUPPLEMENTARY NOTES			
19. KEY WORDS (Continue on reverse side if necessary and identify by block number) X-Ray Hydrodynamics Laser Propagation			
20. ABSTRACT (Continue on reverse side if necessary and identify by block number) The disturbance produced in a gaseous medium by the absorption of an intense, narrow pulse of x-rays is such that the absorption of later x-rays which follow the same path is greatly reduced. Various processes which affect this absorption reduction have been investigated and a numerical technique has been employed to obtain quantitative predictions of the range.			

DD FORM 1473
1 JAN 73

EDITION OF 1 NOV 65 IS OBSOLETE

UNCLASSIFIED

SECURITY CLASSIFICATION OF THIS PAGE (When Data Entered)

TABLE OF CONTENTS

	Page
LIST OF ILLUSTRATIONS	5
I. INTRODUCTION	7
II. ELEMENTARY CONSIDERATIONS	8
III. NUMERICAL TECHNIQUE	10
IV. MATHEMATICAL FORMULATION	11
A. Photoelectric Effect	11
B. Energetic Electron Energy Loss	14
C. Compton Effect	16
D. Mass Motion	17
E. Other Processes	19
V. PRELIMINARY RESULTS	22
VI. SUMMARY	27
REFERENCES	29
DISTRIBUTION LIST	33

LIST OF ILLUSTRATIONS

Figure	Page
1. Graphic representation of the problem. Part (a) shows a longitudinal (temporal) profile of an x-ray pulse and part (b) shows a radial profile. The pulse is then a long, thin sliver and we consider its propagation successively through short intervals as shown in part (c).	12
2. X-ray pulse shape and some resulting ion densities within the beam as a function of time for the initial propagation interval	23
3. Remaining pulse energy versus propagation distance in the effusion approximation	25
4. Temperature versus time in the effusion approximation within the beam (region M) and surrounding the beam (region W).	25
5. Radial mass density (relative to STP air) distribution at two times for the laser parameters given in Table I. Times t_1 and t_2 are 80 ns and 60 ns, respectively, before the arrival of the x-ray pulse peak. The radial x-ray pulse shape is uniform and extends to $r = 5 \mu$	26
6. Same type of plot as Figure 5 except that the radial pulse shape is Gaussian with a full width at half maximum of 10μ	28

PRECEDING PAGE BLANK-NOT FILMED

I. INTRODUCTION

Since its birth less than twenty years ago, modern laser technology has been following a natural evolutionary path to higher powers and shorter wavelengths. Single laser pulses with energies of hundreds of joules are now available^{1,2} and laser action has been observed in the vacuum ultra-violet region of the electromagnetic spectrum³. Efforts are also being made to observe lasing of x-rays⁴⁻⁹. The characteristics of possible x-ray lasers are discussed in Reference 10 which concludes that early devices will have diameters of a few microns, short pulse lengths (10^{-13} to 10^{-15} seconds), and low powers. More recently, means to achieve longer pulses have been identified¹¹.

1. T. F. Stratton, "A High Energy, Short Pulse CO₂ Laser System", VIII International Quantum Electronics Conference, San Francisco, CA, June, 1974, Abstract B.2.
2. A. Crocker, H. M. Lambertson, E. W. Parcell and H. C. Probyn, "500 J CO₂ Electron Beam Laser Controlled by a Glow Discharge Electron Gun", VIII International Quantum Electronics Conference, San Francisco, CA, June, 1974, Abstract B.4.
3. A. Wayne Johnson and J. B. Gerardo, "The Vacuum-Ultra-Violet Xenon Laser", VIII International Quantum Electronics Conference, San Francisco, CA, June, 1974, Abstract M.2.
4. M. A. Duguay and P. M. Rentzepis, "Some Approaches to Vacuum UV and X-Ray Lasers", Appl. Phys. Letters, Vol. 10, 350 (1967).
5. R. C. Elton, R. W. Waynant, R. A. Andrews, and M. H. Reilly, "X-Ray and Vacuum-UV Lasers", NRL Report 7412, May, 1972.
6. P. J. Mallozzi, et al., "X-Ray Emission from Laser-Generated Plasmas", ARPA Technical Report 1723, January, 1972.
7. M. O. Scully, W. H. Louisell, and W. B. McKnight, "A Soft X-ray Laser Utilizing Charge Exchange", VIII International Quantum Electronics Conference, San Francisco, CA, June, 1974, Abstract M.9.
8. R. A. McCorkle and J. M. Loyce, "Threshold Conditions for Amplified Spontaneous Emission of X-Radiation", Phys. Rev. A., Vol. 10, 1974, p. A903.
9. J. G. Kepros, E. M. Eyring, F. W. Cagle, Jr., "Experimental Evidence of an X-Ray Laser", Proc. Nat. Acad. Sci. USA, Vol. 69, 1972, p. 1744.
10. R. A. Andrews, "X-Ray Lasers-Current Thinking", NRL Memorandum Report 2677, October, 1973.
11. R. C. Elton, "Analysis of X-Ray Laser Approaches: 2. Quasi-stationary Inversion on K α -Innershell Transitions", NRL Memorandum Report 2906, October, 1974.

There are intriguing applications for an x-ray laser. Reference 10 lists and discusses a number of these ranging from basic physics research to medical studies but concludes that, at least for early devices, x-ray lasers will have their greatest impact on material science and related fields. Some applications, however, would require the beam to propagate a significant distance through air.

Unfortunately, air is not transparent to soft x-ray photons as it is for optical photons. In fact, the range of individual 10-keV x-rays in air is only about 2 meters and at 1 keV the range is smaller by a factor of 1000. However, these ranges are appropriate only for x-rays which have a negligible effect on the medium through which they propagate. If the diameter of the beam is sufficiently small and the intensity sufficiently high, then the x-rays will have a drastic effect on the air. In fact, there are several effects produced which will extend the range. This study is being made to quantify these effects and determine x-ray laser parameters which maximize the range.

II. ELEMENTARY CONSIDERATIONS

When a narrow collimated beam of soft x-rays propagates through matter it is attenuated exponentially by absorption and scattering processes. The former is due mainly to the photoelectric effect which results in the ejection of an electron from the absorbing atom, usually from an inner shell. The atom then promptly fills this vacancy with an electron from an outer shell and the excess energy is emitted either as an x-ray or, as is usually the case with atmospheric gases, in the kinetic energy of an Auger electron. The resulting ion, which in the case of an Auger transition is twice ionized, may repeat the process and thereby become four times ionized. For nitrogen ($Z=7$), further photoelectric absorption is accompanied by an x-ray rather than an Auger emission so that the successive absorption by an atom of five x-rays can completely strip the atom of electrons. Further photoelectric absorption by this ion does not occur until it recombines with a free electron, and this occurs on a time scale greater than probable pulse widths.

This stripping process is therefore one means for reducing the amount of photoelectric absorption, which is the most important absorptive interaction for soft x-rays. Furthermore, the amount of energy expended by the pulse to produce this stripping can be made small by making the pulse diameter small. This not only reduces the number of air molecules in the path of the pulse, but also reduces the distance that an ion must travel as a result of thermal motion in order to leave the path of the pulse. This thermal motion is important because the heating is confined to a small region surrounding the beam and is greatest within the beam. This results in a large radial pressure gradient which rapidly removes particles from the path of the pulse because its radius is very small. If the x-ray pulse has the optimum shape in time, this removal of absorbing atoms can occur before the arrival of the main part of the pulse, so that very few atoms must be fully stripped to eliminate photoelectric absorption.

When an energetic photoelectron is produced it starts away from the atom in a direction which would quickly remove it from the path of the pulse. The actual path of the electron, however, is a tortuous one because it can suffer large energy and momentum changes with each collision. Even so, if the air is relatively undisturbed then the range of these electrons is considerably greater than the pulse radius. As the air then becomes slightly ionized there will be an electric field produced as a result of the charge distribution which can roughly be described as a small-diameter cylinder of high density positive charge surrounded by a large-diameter cylinder of low-density negative charge. The force exerted by this field on the energetic photoelectrons opposes their outward motion. A force is also exerted on the positive ions driving them radially outward. The resulting motion is a damped plasma oscillation which quickly absorbs the excess kinetic energy of any charged particles, but also raises the temperature and thereby leads to a reduction of the number of absorbing atoms that the x-ray pulse encounters, because the net flow of particles is radially outward. There are thus at least three processes which serve to reduce the amount of photoelectric absorption, which normally limits the range of 10-keV x-rays, for example, to about two meters.

But, even if photoelectric absorption can be neglected completely, the range of x-rays is still limited to about forty meters by the Compton effect, which is scattering of x-rays by free or loosely-bound electrons. However, the processes which reduce the amount of photoelectric absorption also affect the amount of Compton absorption. The stripping of the electrons from the atoms actually increases slightly the amount of Compton absorption. On the other hand, if the net hydrodynamic and electrodynamic motion of the positive ions is radially outward then the electrons can't be far behind because they are much lighter and can be easily pulled along as the plasma tries to restore charge neutrality. There is thus a conceivable means for reducing both photoelectric and Compton losses.

What, then, ultimately limits the range of intense x-ray pulses? As it turns out, the pulse diameter must be quite small in order to reduce photoelectric and Compton absorption to insignificance. Just how small it must be is determined by how efficient the hydrodynamic and electrodynamic motion is at removing absorbers from the pulse path. The accuracy of such a prediction depends strongly on how well these processes are described mathematically and computationally. Although the formulation of a solution to these problems is far from complete it is already apparent that the pulse diameter cannot be greater than about 10^{-4} meters. But even if the diameter is this large, the inherent divergence of the pulse is enough to reduce the intensity of a 10-keV x-ray pulse by a factor of 4 as it propagates 100 meters. This increase of the diameter of the pulse reduces the rate at which absorbers move out of the path of the pulse, and eventually the diameter gets so large and the intensity so low that the remainder of the range is equal to the normal range of these x-rays in air, which is less than two meters.

On the other hand, this may not be the ultimate limit at all if something happens, or can be made to happen, which focusses the x-ray beam. Certainly large deflections are not possible but, as we will see, they are not needed. The divergence angle which must be overcome is only about 10^{-4} to 10^{-6} radians. Because of motion of ions and electrons radially outward, the late part of the x-ray pulse will "see" mostly empty space, or a vacuum, which has a refractive index of unity. The region surrounding the late part of the pulse will have an index of refraction which, if it is equal to that for normal air, can produce total reflection of x-rays incident on a sharp interface at the divergence angle. The complete description of the conditions required for such whole-beam self-focussing is a truly ambitious undertaking and has not yet been quantitatively developed, but the possibility of such an effect justifies the investigation of the propagation characteristics of non-diverging x-ray beams.

III. NUMERICAL TECHNIQUE

Because of the relatively short lifetimes of x-ray emitting species and the difficulty of making mirrors for x-rays, it is probable that early-generation x-ray lasers will operate in a pulsed mode. Furthermore, higher powers are possible in this mode and we anticipate that these will be needed to significantly extend the range. We therefore wish to consider the passage of a cylindrical, narrow-diameter, finite-length x-ray pulse through a medium. Since air is mostly nitrogen and oxygen and the atomic properties of these are very similar, we will approximate the air by pure nitrogen gas. For the numerical treatment, the pulse is divided into a number of sub-pulses, each of which has only a minor effect on the propagation medium. The problem then is to determine the amount of attenuation suffered by each sub-pulse. This attenuation will vary not only with the distance along the length of the pulse but also with the distance radially from the axis of symmetry. Furthermore, all of these vary with the distance the pulse has propagated.

Since the changes in the attenuation are caused by changes in the propagation medium it is obvious that the medium must be described by some sort of computational grid. The crucial question is whether this grid must be two- or three-dimensional, for if the computer must simultaneously keep track of the condition of the medium along the entire length of the pulse the memory and computation time required would be very great. Fortunately a two-dimensional grid is sufficient for the x-ray energies and pulse diameters with which we are concerned. This is true because mass motion parallel to the direction of propagation is negligible. This follows from the fact that the temperature along the propagation direction changes more slowly with distance than that in the transverse direction. Furthermore, the area of the surface through which these mass flows occur is much smaller for flows parallel to the propagation direction. Figure 1(a) shows an assumed longitudinal x-ray pulse intensity profile and its approximate representation as a

series of square sub-pulses. Similarly, Figure 1(b) shows a transverse intensity profile which extends out to some maximum radius r_m . The actual shape of the region of space over which the intensity is constant is a long, thin cylindrical shell. The entire pulse then looks like a long, thin sliver and we consider its propagation successively through short intervals as shown in Figure 1(c).

We will consider the propagation of the entire pulse, one small section at a time, through an interval of length ℓ . With the passage of each of these sub-pulses a number of fundamental interactions will be produced which alter the condition of the medium contained in this cylinder. This cylinder is divided into many cylindrical shells of equal thicknesses Δr and outer radii r_i . During a subpulse the motion of matter between these cylindrical shells is calculated from their thermodynamic properties assuming the material is an ideal gas. The largest r_i is chosen so that the disturbance in the medium reaches the outermost cylindrical shell only after the last sub-pulse has passed. The length of the propagation interval, ℓ , is chosen so that the overall pulse shape does not change greatly from one interval to the next. Similarly, the size of the subpulses is chosen small enough so that the medium does not change greatly during a single subpulse. These subpulses must be smallest where the absorption is greatest along the pulse, and the relative position of this maximum-absorption region within the pulse moves as the pulse propagates. When calculations are made away from this region several subpulses are combined to reduce computation time.

IV. MATHEMATICAL FORMULATION

A. Photoelectric Effect

The photoelectric effect is responsible for the severe attenuation of soft x-ray beams in matter. In this process the x-ray energy is transferred to a bound electron, forcibly ejecting it from the atom or ion. The resulting ion may subsequently absorb more x-rays by the same process until all of its electrons have been removed. Photoabsorption may, of course, occur for electrons in the K-shell or in the L-shell. For (nitrogen) neutral atoms, photoabsorption by K-shell electrons is about twenty times more probable. Since 1s orbitals are not very sensitive to the occupancy of 2S or 2P orbitals, the cross section for K-shell photoabsorption can be assumed to be constant for atoms and ions except when the K-shell contains less than two electrons¹². The L-shell cross sections, however,

¹². D. W. Missavage and S. T. Manson, "Photoionization of Positive Ions of Atomic Oxygen", Phys. Letters, Vol. 38A, 1972, p. 85.

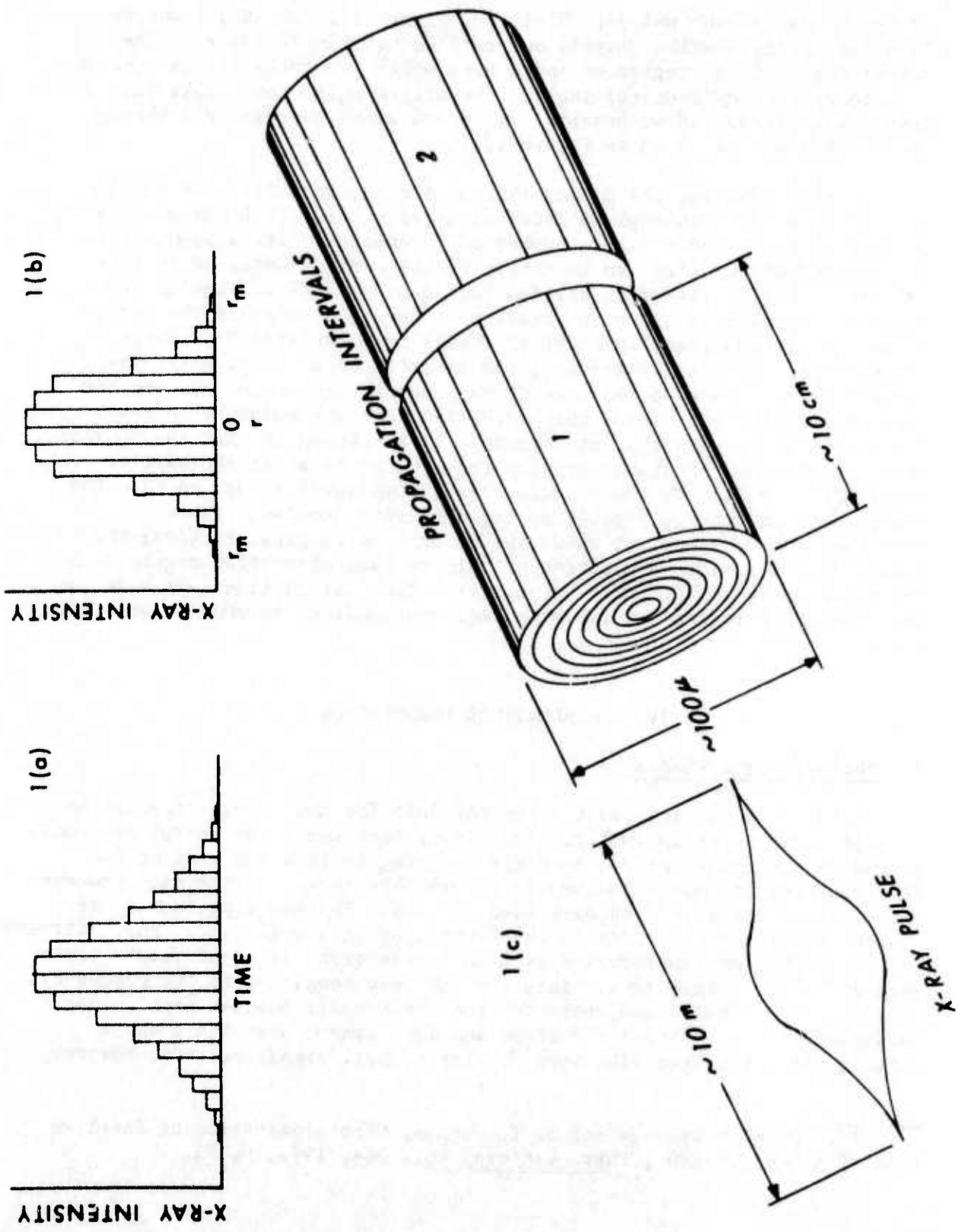


Figure 1. Graphic representation of the problem. Part (a) shows a longitudinal (temporal) profile of an x-ray pulse and part (b) shows a radial profile. The pulse is then a long, thin sliver and we consider its propagation successively through short intervals as shown in part (c).

do vary with the degree of ionization and are scaled from the neutral atom values by using Slater's rules for the screening potential¹³. For absorption by electrons in the L-shell the effective charge Z_{eff} is

$$Z_{\text{eff}} = Z - Z_k(0.85) - Z_L(0.35),$$

where Z is the nuclear charge, and Z_k and Z_L are the number of electrons in the K- and L-shell, respectively. For the x-ray energies we consider we will determine the ion cross section per L-electron from the neutral atom cross section assuming that the cross section is proportional to Z_{eff}^4 .

For each type of absorption we will assume that each subpulse is absorbed exponentially as it propagates through the distance ℓ so that

$$N = N_0 e^{-\mu\rho\ell},$$

where N_0 is the initial number of x-ray quanta in the subpulse, N is the number remaining, μ is the photoabsorption cross section, and ρ is the density of species in the medium for which the absorption is being calculated. We further assume that the medium is pure nitrogen gas and that the molecular bond is broken with the first photoabsorption. Thus for each element of the cylindrical grid we will keep track of the densities of nine different species: free electrons, neutral atoms, and ions with charges from $1+$ to $7+$. The cross sections for neutral atoms are taken from analytical approximations to experimental values¹⁴ which are efficient for computer use.

The number of photoelectrons produced in a pathlength ℓ is thus $(N_0 - N)$ regardless of which component is responsible for the absorption. The energies of these electrons will, however, depend upon the degree of ionization of the absorber since the electron energy is

$$E = h\nu - B,$$

where $h\nu$ is the x-ray photon energy and B is the binding energy of the electron and varies with the shell and number of electrons on the ion. For low energy such that $\beta = v/c$ for the ejected electron is small, theory and experiment are in agreement in giving a distribution in solid angle of the direction of ejection of the photoelectrons proportional to

13. M. D. Torrey, N. A. Zessoules, and W. D. Lanning, "Numerical Simulation Techniques for Nonequilibrium Effects of High-Altitude Nuclear Detonations", Technical Operations Research, Report No. TO-B 66-29, May, 1966.

14. F. Biggs and R. Lighthill, "Analytical Approximations for X-Ray Cross Sections II", Sandia Laboratories, Report No. SC-RR-71 0507, December, 1971.

$\cos^2\psi$, where ψ is the angle between the direction of ejection and the electric vector of the photon¹⁵, which is perpendicular to the propagation direction. We will simply assume that all photoelectrons are emitted in the most probable direction, which is radially outward from the x-ray path. We also assume that each ion is in its ground state before the absorption and returns to the ground state of the new ion promptly after the absorption. Since the fluorescence yield of nitrogen is only about .006¹⁶, this is tantamount to assuming that an Auger emission promptly follows the K-shell absorption by ions which have four or more electrons and that a low-energy x-ray is promptly emitted after a three-electron ion absorbs an x-ray in the K-shell. The energy of Auger electrons is, to a good approximation,

$$E = W(K) - 2 W(L),$$

where $W(K)$ is the energy of the ion in which a K-electron is missing and $W(L)$ is the energy if an L-electron is missing¹⁷. The energy of the Auger electrons is much less than that of the photoelectrons and results in heating much closer to the propagation path.

B. Energetic Electron Energy Loss

When an atom or ion absorbs an x-ray via the photoelectric effect, the x-ray disappears completely and its energy is transferred to a bound electron. Part of this energy is transferred to the ion as its bond with the electron is broken. The remaining energy is carried by the photoelectron as kinetic energy and is deposited in the medium some distance from where the primary interaction occurred. The size of the region where the photoelectron loses its energy and the manner in which it does so depends upon the condition of the medium. When the medium is in its initial state this energy loss proceeds by a well-understood mechanism and has been extensively studied experimentally. However, as the air becomes ionized and the charge separation begins to produce an electric field, the energy-loss mechanism is not so clear and experimental data is not available. On the other hand, some simplifying assumptions can be made which lead to a representation of the problem which is amenable to a computer calculation.

15. A. H. Compton and S. K. Allison, X-Rays in Theory and Experiment, Van Nostrand, Princeton, N.J., 1935, pp. 564-582.

16. W. Bambynik, B. Craseman, R. W. Fink, H. U. Freund, H. Mark, C. D. Swift, R. E. Price, and P. V. Rao, "X-Ray Fluorescence Yields, Auger, and Coster-Kronig Transition Probabilities", Rev. Mod. Phys., Vol. 44, 1972, p. 716.

17. E. U. Condon, "X-Rays", in Handbook of Physics edited by E.U. Condon and H. Odishaw, McGraw-Hill, New York, 1958, p. 7-124.

In a relatively undisturbed medium energetic electrons lose energy primarily via ionizing collisions with neutral atoms. The energy loss per unit path length for this process is given by¹⁸

$$\left(\frac{dT}{dS}\right)_{\text{ion}} = 4\pi r_0^2 \frac{M_0 c^2}{\beta^2} NZ \left[\ln \beta \left(\frac{T+M_0 c^2}{I} \right) \left(\frac{T}{M_0 c^2} \right)^{1/2} - \frac{\beta^2}{2} \right] \quad (1)$$

where $r_0 = \frac{e^2}{M_0 c^2} =$ classical electron radius

$$4\pi r_0^2 = 1.00 \times 10^{-24} \text{ cm}^2/\text{electron} = 1.00 \text{ barn/electron}$$

$$M_0 c^2 = 0.51 \text{ MeV} = \text{electron rest energy}$$

$$\beta^2 = (v/c)^2 = 1 - [(T/M_0 c^2) + 1]^{-2}$$

NZ = bound electron density

I = geometric mean ionization and excitation potential

The energy I can be written

$$Z \ln I \equiv \sum_{n,1} f_{n,1} \ln A_{n,1} \quad (2)$$

where $f_{n,1}$ is the sum of the oscillator strengths for all optical transitions of the electron in the $n,1$ shell and is close to unity while $A_{n,1}$ is the mean excitation energy of the $n,1$ shell and can be put equal to the ionization potential with sufficient accuracy. Theoretical values of I, calculated with hydrogen-like wave functions, are of little practical value. But empirical values of I determined for each value of Z can be used to accurately predict the energy loss in unionized matter¹⁹.

However, in the problem at hand, we must be concerned also with the further ionization of ions. The value of I will certainly be different for these, no experimental measurements are available, and no rigorous prescription exists for determining I. But rather than neglect the variation of I with the state of ionization, we shall employ equation (2) taking $f_{n,1} = 1$, $A_{n,1} =$ ionization potential, and summing only over those electronic states occupied when the ion is in its ground state.

¹⁸. R. D. Evans, The Atomic Nucleus, McGraw-Hill, New York, 1955, p. 532.

¹⁹. Ibid, p. 580.

For nitrogen, this results in values for I ranging from 670 eV for the 6+ ion to 92 eV for neutral atoms. This can be compared to the experimental value for neutral nitrogen which is 80.1 eV²⁰.

As the medium becomes ionized the free electron density increases and energetic electrons will lose energy in collisions with these. Following the approach taken by Richards²¹, we will write the energy loss for fast electrons in a plasma as

$$\frac{dE}{dX} = n_e \phi_c E/4 + \sum_i \left(\frac{dT}{dS} \right)_{ion}^{(i)} + \left(\frac{dE}{dX} \right)_{exc}, \quad (3)$$

where the first term accounts for the energy lost by electrons to other electrons; n_e is the free electron density and ϕ_c is the Coulomb cross section, given approximately by $\pi(e^2/E)^2$. The second term is the sum of the energy losses due to ionizing collisions with each ionic species computed from equation (1). The last term accounts for short-range collisions and for excitations of the ions and is assumed to be equal to the middle term, as it is for neutral gases.

Another phenomenon with which we must be concerned is the conversion of the kinetic energy of photoelectrons to potential energy in an electric field. Although this is an important effect, its rigorous inclusion would complicate and greatly increase the computation time of the problem. The effect of this phenomenon will be to confine the region of photoelectron energy loss to the immediate vicinity of the plasma-which in turn will be near the beam. In order to account for this at least in an approximate way, we will assume that photoelectrons lose their energy in the cylindrical shell in which they are produced.

C. Compton Effect

The Compton effect produces both scattering and absorption. That is, part of the energy of the affected photons is transferred to the responsible electron and adds to the thermal energy. However, most of the energy is scattered and the photon has no further appreciable effect on the medium. This loss mechanism therefore can use up large amounts of the x-ray pulse energy and limit the range to about 40 meters.

20. Kai Siegbhan, Alpha-, Beta-, and Gamma-Ray Spectroscopy, North-Holland, Amsterdam, 1966, p. 26.

21. P. I. Richards, "Summary Report on Investigation of Radiation and Chemical Calculations", Technical Operations Research, Report No. TO-B 62-24, May, 1962.

However, if the photoelectric range is considerably less than the Compton range, then the medium can be greatly disturbed before Compton losses become important. If the nature of the disturbance is to reduce the electron density in the vicinity of the beam, then Compton losses can be reduced.

The average Compton collision cross section is given by

$$e\sigma \approx \frac{8\pi}{3} r_0^2 (1 - 2\alpha + 5.2\alpha^2 - 13.3\alpha^3 + \dots) \quad (4)$$

for small $\alpha = \frac{h\nu_0}{M_0c^2}$, where $h\nu_0$ is the x-ray energy and M_0c^2 is the electron rest energy²². This cross section is the probability for removal of a photon from a collimated beam while passing through an absorber containing one electron/cm². The average Compton absorption cross section is given by²³

$$e\sigma_a \approx \frac{8\pi}{3} r_0^2 (\alpha - 4.2\alpha^2 + 14.7\alpha^3 - \dots) \quad (5)$$

The average energy removed from an incident beam by Compton collisions is measured by $e\sigma$ while the average energy absorbed by the electrons is measured by $e\sigma_a$. The average energy of a Compton electron is then

$$T_{av} = \frac{e\sigma_a}{e\sigma} h\nu_0 \quad (6)$$

This amount of energy will be added to the total thermal energy for each Compton electron and will thus appear directly as heat. Other explicit processes which contribute directly to the thermal energy include recoil of an ion with photoelectron emission, energy transferred in photoelectron-thermal electron collisions, and the energy of photoelectrons which is less than the lowest ionization potential but greater than the thermal energy.

D. Mass Motion

The absorption by a medium of a narrow x-ray beam quickly produces a cylinder which has a large radial temperature gradient and a negligible axial temperature gradient. The resulting mass motion is of utmost importance since it removes absorbing particles from the path of the beam. For small beam diameters this can occur rapidly enough for the resulting range to be considerably greater than it would be otherwise.

22. R. D. Evans, op. cit., p. 684.

23. Ibid, p. 688.

In the limit as one goes to smaller beam diameters and shorter pulse widths this mass motion changes from a hydrodynamic flow to an effusion flow because the heated ions can move distances significant compared to the beam diameter before they equilibrate with the surrounding medium. One may then assume that the heated region is a radially expanding cylinder with its escaping particles effusing into the surrounding medium and gradually raising its temperature. Calculations have been made with this approximation and the results are given in the next section.

A more exact representation of the mass motion can be made by including the physics of fluid flows. Following a method used to describe explosive hydrodynamics²⁴, we employ a finite-difference approximation to the differential equations which expresses the basic physical limitations on the flow without introducing spurious, unstable processes through the numerical approximations.

The fundamental physical laws of fluid flow are conservation of mass, momentum, and energy. The state of the fluid can be specified with the densities of each of these quantities. The conservation laws are imposed by requiring that flows out of one cell of the computational grid must reappear in another. This is most easily ensured by focussing attention on the flows across the faces between grid cells. Computing these interfacial flows for the mass essentially evaluates $\nabla \cdot (\rho \vec{v})$, where ρ is the mass density and \vec{v} is the fluid flow velocity. Crediting and debiting these flows, for a brief step forward in time, essentially sets

$$\frac{\partial \rho}{\partial t} = -\nabla \cdot (\rho \vec{v}), \quad (7)$$

which expresses the law of conservation of mass.

A corresponding treatment for the energy expresses

$$\frac{\partial E}{\partial t} = -\nabla \cdot [(E+p)\vec{v}] \quad (8)$$

where p is the pressure and $E = \epsilon + \frac{\rho v^2}{2}$, (9)

ϵ is the thermal energy density, and E is the total energy density. Gravity is neglected and the term $\nabla \cdot (p\vec{v})$ accounts for the work done by compression and by streaming against the local pressure gradient. The net result is that one must evaluate interfacial flows of the quantity $E+p$.

²⁴. P. I. Richards, "The Tech/Ops Two-Dimensional Time-Dependent Hydrodynamics Code", Technical Operations Research, Report No. TO-B 62-22, April, 1962.

Since the axial motion is ignored, the momentum conservation law is expressed as

$$\frac{\partial(\rho v_r)}{\partial t} = -\nabla \cdot [(\rho v_r) \vec{v}] - \frac{\partial p}{\partial r} . \quad (10)$$

A straightforward time integration of the form

$$y(t+\Delta t) = y(t) + \frac{dy}{dt} \Delta t \quad (11)$$

is used to determine the changes in the mass, energy, and momentum densities. The size of the time steps Δt corresponds to the widths of x-ray sub-pulses and must be small enough so that the maximum signal velocity times Δt is small compared to the computational grid dimension.

E. Other Processes

Multiple ionization may occur following K-shell photoelectric absorption due to a process called electron shake-off. This is the phenomenon by which an electron in a given orbital is excited into a new orbital or into the continuum as the result of a sudden change in the central potential. Since the potential seen by the electron is made up of the nuclear charge minus the shielding of the other electrons, electron shake-off may be initiated either by a sudden change in the nuclear charge, as in β -decay, or a sudden change in the electron configuration, as in photoionization. The most successful treatment of electron shake-off has been through the use of the sudden approximation and theoretical shake-off probabilities following β -decay have been calculated for many elements²⁵. However, calculations have not been made for the particular case in which we are interested: shake-off following photoionization in nitrogen. The nearby element neon, however, has been studied extensively^{26,27} and experimental data is also

25. T. A. Carlson, C. W. Nestor, Jr., T. C. Tucker, and F. B. Malik, "Calculation of Electron Shake-off for Elements from Z=2 to 92 with the use of Self-Consistent-Field Wave Functions", Phys. Rev., Vol. 169, 1968, p. 27.

26. T. A. Carlson and M. O. Krause, "Experimental Evidence for Double Electron Emission in an Auger Process", Phys. Rev. Letters, Vol. 14, 1965, p. 390.

27. M. O. Krause, M. L. Vestal, W. H. Johnston, and T. A. Carlson, "Readjustment of the Neon Atom Ionized in the K Shell by X-Rays", Phys. Rev. A, Vol. 133, 1964, p. A385.

available for the dependence of the shake-off probability on the photoelectron energy²⁸. The combined probability for the shake-off of one or more electrons in addition to the photoelectron and Auger electron is about 25.4% for a photoelectron energy of 7.5 keV.

The ionization potential of an ion in a plasma is not the same as that of an isolated ion but is reduced because of plasma polarization²⁹. At the position of an ion with ionic charge equal to R times the electronic charge, the average potential from all other charged particles in the system is obtained from an approximate solution of Poisson's equation and is³⁰

$$J(R) = \theta [2 (Z^* + 1)]^{-1} \{ [3(Z^* + 1) K(R) + 1]^{2/3} - 1 \}, \quad (12)$$

where θ is the temperature in energy units. The other quantities appearing in equation (12) are defined in terms of the average electron density N_e and the average density N_R of ion species with charge R ,

$$Z^* = \frac{\overline{Z^2}}{Z} = \frac{\sum_R N_R R^2}{N_e} \quad (13)$$

$$K(R) = R e^2 / (D \theta) \quad (14)$$

$$D^{-2} = 4 \pi N_e e^2 (1 + Z^*) / \theta \quad (15)$$

It has been pointed out³¹ that this approximation is not thermodynamically consistent but can be made so by replacing $J'(R)$ by

$$J(R) = (R/\overline{Z}) J'(\overline{Z}). \quad (16)$$

The ionization potential of an ion of charge R in the plasma is then lower than that of an isolated ion by the amount

28. T. A. Carlson and M. O. Krause, "Electron Shake-off Resulting from K-Shell Ionization in Neon Measured as a Function of Photoelectron Velocity", Phys. Rev. A, Vol. 140, 1965, p. A1057.

29. Howard D. Cohen, Donald E. Parks, and Albert G. Petschek, "A Study of Equations of State/Opacity of Ionized Gases", SYSTEMS, SCIENCE and SOFTWARE, Report No. DASA 2597-1, April, 1971.

30. J. C. Stewart and K. D. Pyatt, "Lowering of Ionization Potentials in Plasmas", Ap. J., Vol. 144, 1966, p. 1203.

31. D. E. Parks, G. Lane, J. C. Stewart, and S. Peyton, "Optical Constants of Uranium Plasma", NASA Report No. CR-72348 [GA8244], 1967.

$$\Delta I_R = (R+1)J(\bar{Z}),$$

where

$$\bar{Z} = N^{-1} N_e$$

$$\bar{Z}^2 = N^{-1} \sum_R N_R R^2$$

and

$$N = \sum_R N_R.$$

Electron-ion recombination and the resulting radiation can alter the absorption characteristics for long width pulses. This process leads to the reappearance of photoelectric absorbers on a time scale determined by the recombination coefficient, theoretical expressions for which are given by Spitzer³². These theoretical values, however, are usually many orders of magnitude smaller than measured values in laboratory plasmas. This apparent discrepancy may be attributed to a different type of recombination process^{33,34} in which a molecular ion captures an electron and dissociates into two neutral atoms. Quantum-mechanical calculations predict an electron-ion recombination coefficient of the order of 10^{-12} cm³/sec³⁵. This indicates that recombination needs to be considered for ions which remain exposed to the pulse for periods greater than or about 100 ns. However, for the intensities and densities currently being studied, recombination can be ignored.

Several other phenomena are also not included in the calculation at this stage. Among these are the effects of induced electric and magnetic fields, inverse Bremsstrahlung absorption, beam divergence, and

32. Lyman Spitzer, Jr., Physics of Fully Ionized Gases, Interscience, 1962, p. 150.

33. D. R. Bates, "Electron Recombination in Helium," Phys. Rev., Vol. 77, 1950, p. 718.

34. D. R. Bates, "Dissociative Recombination", Phys. Rev., Vol. 78, 1950, p. 492.

35. E. C. G. Stueckelberg and P. M. Morse, "Computations of the Effective Cross Section for the Recombination of Electrons With Hydrogen Ions", Phys. Rev., Vol. 36, 1930, p. 16.

self-focusing. Although these are not included explicitly, assumptions have been made which are expected to produce results qualitatively similar to those which would be obtained from an exact treatment. In particular, the effect of an electric field would be to greatly shorten the range of photoelectrons ejected radially outward from the beam path. Hence the assumption is made that photoelectrons are absorbed in the computational grid in which they are produced.

The inherent beam divergence, λ , can be large enough to considerably spread the beam when the diameter is very small. If this spread does indeed occur, then the range is greatly reduced from that expected for parallel beams. However, the disturbed medium has characteristics which could lead to confinement of the beam or even whole-beam self-focusing. The density of the medium seen by the latter part of the pulse will be reduced by a factor of $\sim 10^4$. If this can be approximated by a vacuum with an index of refraction of unity, and the surrounding medium could be approximated by normal air with an index of refraction of $1 - 2.33 \times 10^{-9}$ for 10 keV x-rays, then the grazing angle for total reflection at a sharp boundary would be $\sim 10^{-4}$. The diffraction-limited divergence λ for this case would be $\sim 10^{-5}$, indicating that x-rays in the latter part of the pulse diverging at this angle would be totally reflected. Until both beam divergence and self-focusing can be included in a consistent manner we will, therefore, consider only parallel or non-diverging beams.

V. PRELIMINARY RESULTS

Calculations have been made with a preliminary version of the computer code for a specific case. The laser parameters and predicted range for this problem are given in Table I. The pulse energy assumed corresponds to about 10% of the maximum energy which can be stored in a normal density solid cylinder of the specified diameter and one meter in length, assuming each atom stores 10 keV. The range here is defined as the distance at which the pulse intensity is attenuated by the factor e^{-1} or the same attenuation factor that an x-ray beam normally experiences in one mean free path. The overall attenuation, however, is not an exponential function of distance but is almost linear.

This result was obtained using the effusion approximation for the transverse motion of ions and electrons. The densities of four of the species as well as the x-ray flux are shown in Figure 2 as a function of time for the initial propagation interval. The x-ray intensity begins abruptly five half-widths (100 ns) before the arrival of the peak and has gaussian shape and is not visible on the linear scale until approximately 50 ns later. The computational grid in this case consists

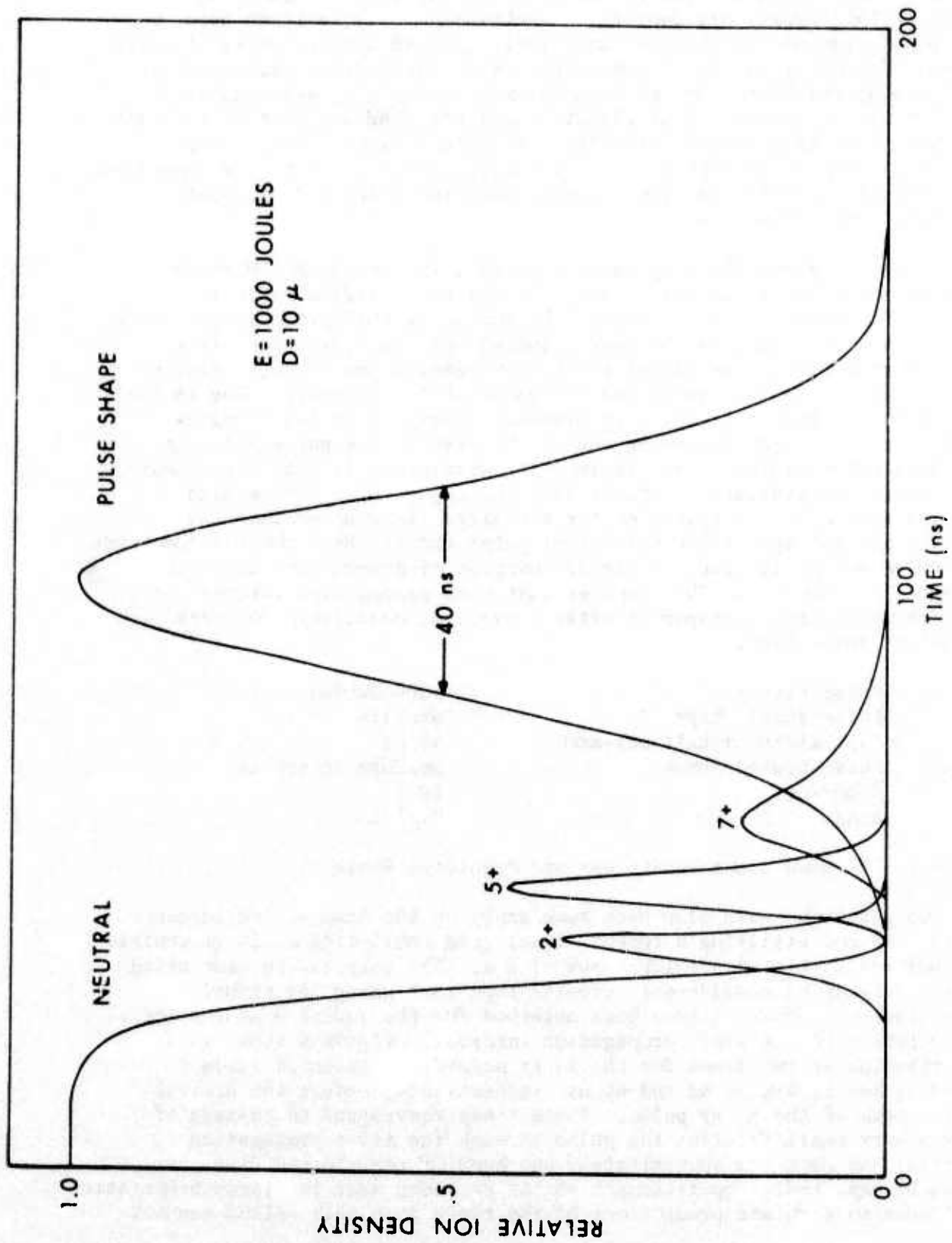


Figure 2. X-ray pulse shape and some resulting ion densities within the beam as a function of time for the initial propagation interval.

of only three zones and the results are for the central zone. As shown in the figure, the density of neutrals rapidly falls to zero, and the population of the various more highly-ionized species peaks at later times. The decay of the 7^+ ionic species is due to mass motion out of the path of the beam. By the time the peak x-ray flux arrives, at $t = 100$ ns, virtually all of the atoms are stripped and most of the ions and electrons have escaped from the beam path thereby reducing the amount of Compton absorption. The resulting range (0.35 km) is therefore considerably greater than the Compton range (0.04 km) and the photoelectric range (0.002 km).

Figure 4 shows the temperature obtained in the central M region through which the x-ray pulse passes and in the W region which is a warm sheath surrounding the beam. The motion of the particles and energy from region to region is obtained assuming that the particles effuse outward at a rate proportional to the ion density and average velocity minus a correction for particles reflected at the boundary. The implicit assumption is made that the high pressure generated in the M region keeps particles from returning and so the results are not applicable for long pulse widths. Another implicit assumption is that the effusing ions move a considerable distance into the region W so that a high density wall does not appear at the boundary. This means that the results are not applicable for larger pulse radii. With these assumptions the pulse energy is almost a linear function of propagation distance, as shown in Figure 3. This implies that each propagation interval in the medium becomes transparent after a certain, relatively constant amount of absorption.

Pulse energy	1000 Joules
Pulse axial shape	Gaussian
Full width at half maximum	40 ns
Pulse radial shape	uniform intensity
Diameter	10 μ
Range	0.35 km

Table 1. Assumed Laser Parameters and Predicted Range.

Calculations have also been made applying the laws of hydrodynamic fluid flow and utilizing a computational grid consisting of 50 concentric cylindrical shells with thicknesses of 1μ . The computation time using this treatment is considerably greater than that using the effusion approximation. Results have been obtained for the radial mass density distribution in the first propagation interval. Figure 5 shows this distribution at two times for the laser parameters given in Table I. Times t_1 and t_2 are 80 ns and 60 ns, respectively, before the arrival of the peak of the x-ray pulse. These times correspond to passage of only a very small fraction the pulse through the first propagation interval and required approximately one hour of computation time. As might be expected, computations have not yet been made for large propagation distances so accurate predictions of the range from this method are not

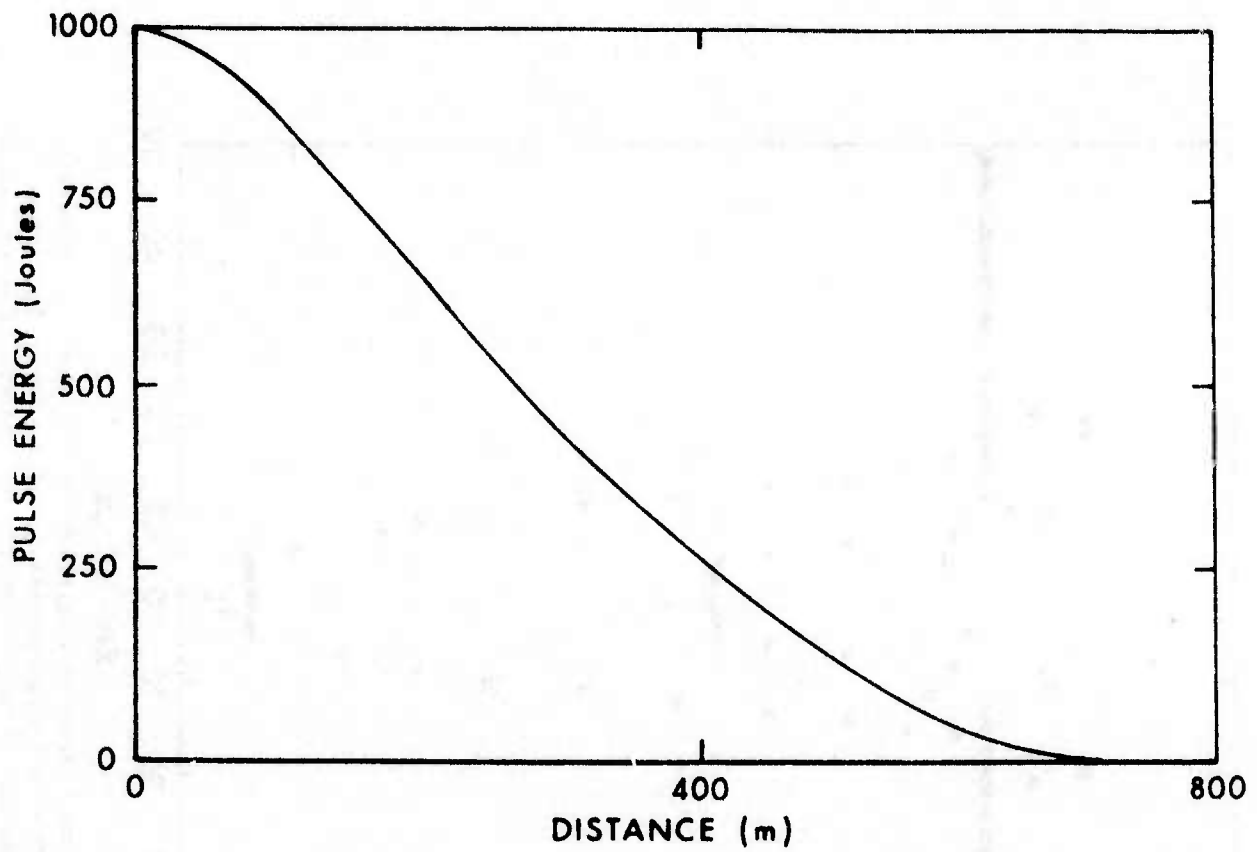


Figure 3. Remaining pulse energy versus propagation distance in the effusion approximation.

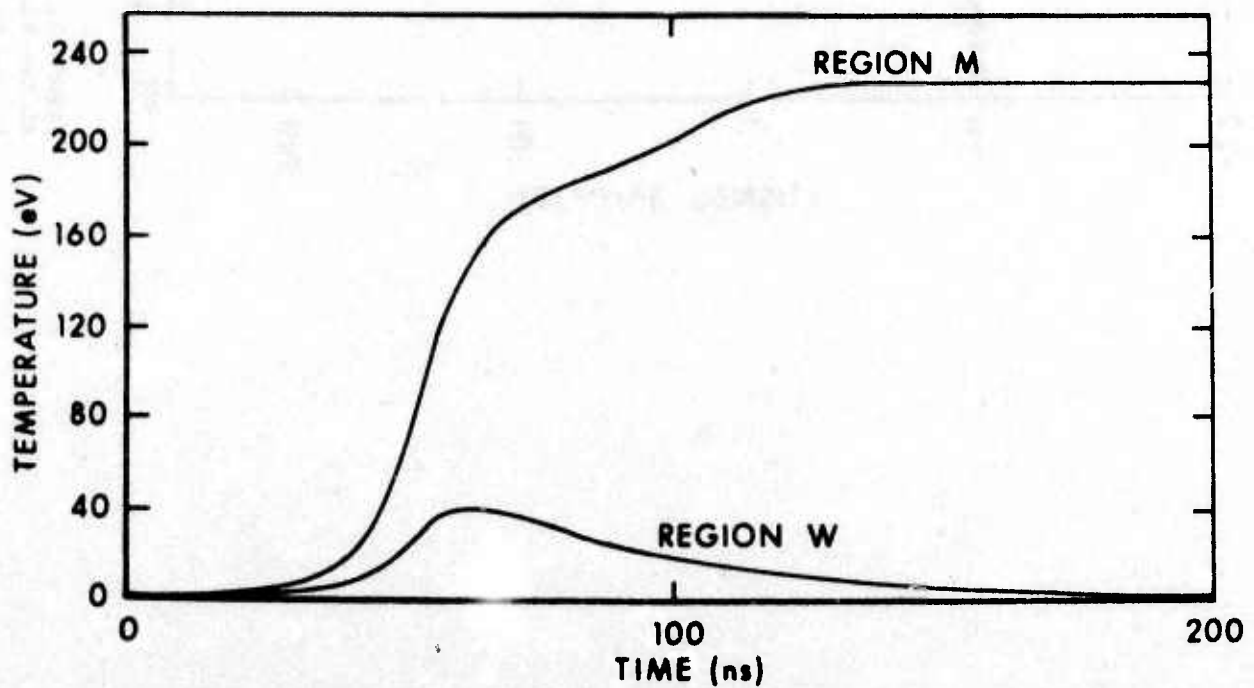


Figure 4. Temperature versus time in the effusion approximation within the beam (region M) and surrounding the beam (region W).

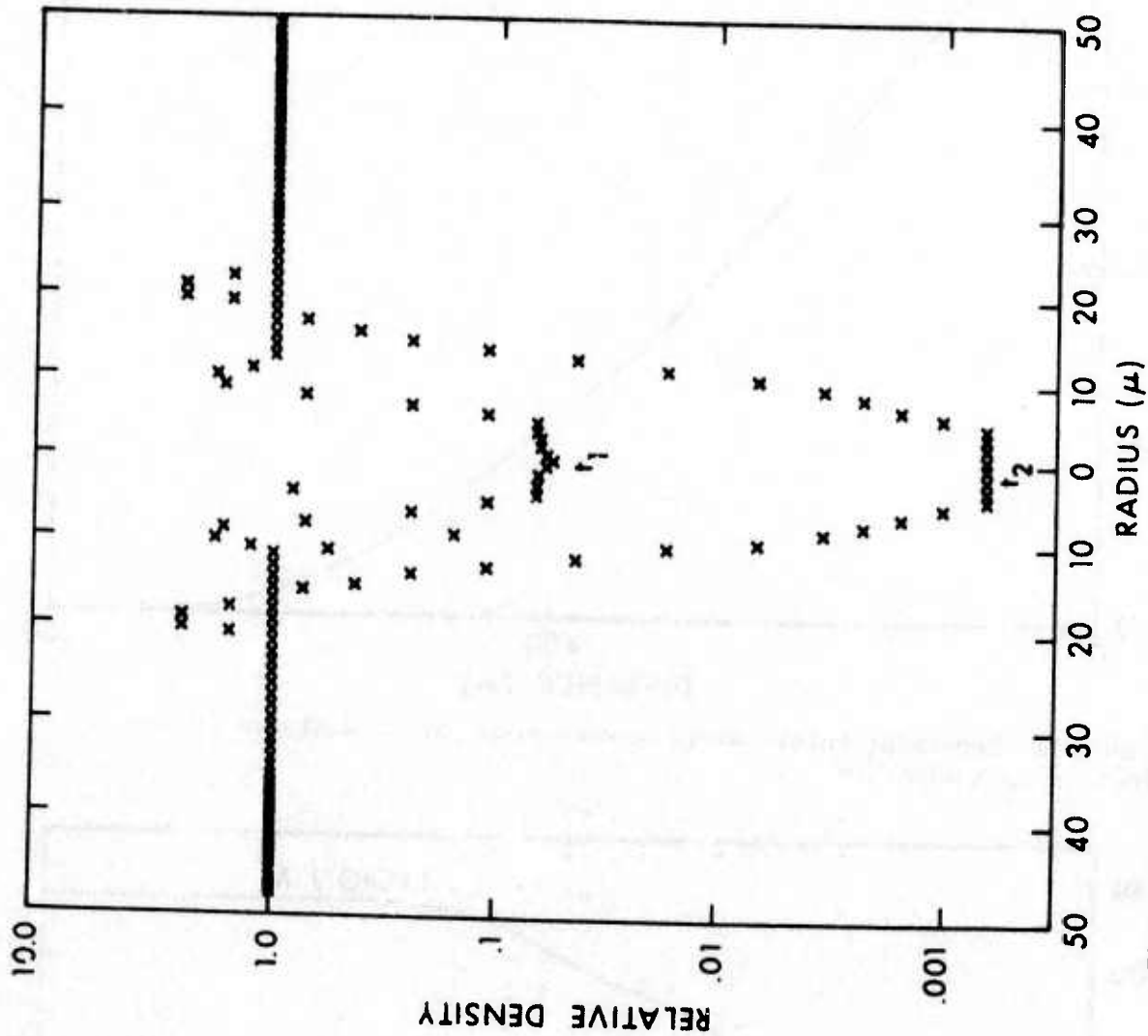


Figure 5. Radial mass density (relative to STP air) distribution at two times for the laser parameters given in Table I. Times t_1 and t_2 are 80 ns and 60 ns, respectively, before the arrival of the x-ray pulse peak. This radial x-ray pulse shape is uniform and extends to $r = 5\mu$.

available. However, since the overall density is reduced by more than three orders of magnitude long before the pulse peak arrives one may expect that the range should be at least 1000 times greater than the normal range, or greater than 2 km.

Figure 6 shows the result of a similar calculation except that the radial pulse shape is taken to be Gaussian with a full width at half maximum of 10 μ . The density reduction at the center is not as great in this case and the range is probably less.

VI. SUMMARY

Several non-linear processes have been discussed which are produced as a result of the propagation of x-rays through air and yet reduce the amount of absorption suffered by later x-rays which travel the same channel. The most important of these processes is the transverse hydrodynamic motion of the gas particles. For typical x-ray pulse parameters the gas particle density can be reduced by an order of magnitude in a few nanoseconds. The efficiency of this density reduction and range extension depends upon the parameters which describe the x-ray pulse.

Future efforts on this study will be aimed at including explicitly the formation of electric fields and their effect on the motion of the photoelectrons and therefore on the size of the region which is heated by the beam. In addition, a method for describing diffraction and refraction of x-rays, similar to methods applied to optical lasers^{36,37}, will be included to determine whether self-focusing can be produced. Finally, calculations will be made for a variety of x-ray pulse parameters to determine the ones which optimize the range.

36. B.R. Suydam, "A Laser Pulse Propagation Code", Los Alamos Scientific Laboratory Report LA-5607-MS, 1974.

37. C.J. Elliot and D.B. Henderson, "A New Technique for Nonlinear Optical Problems", Los Alamos Scientific Laboratory Report LA-5639-MS, 1974.

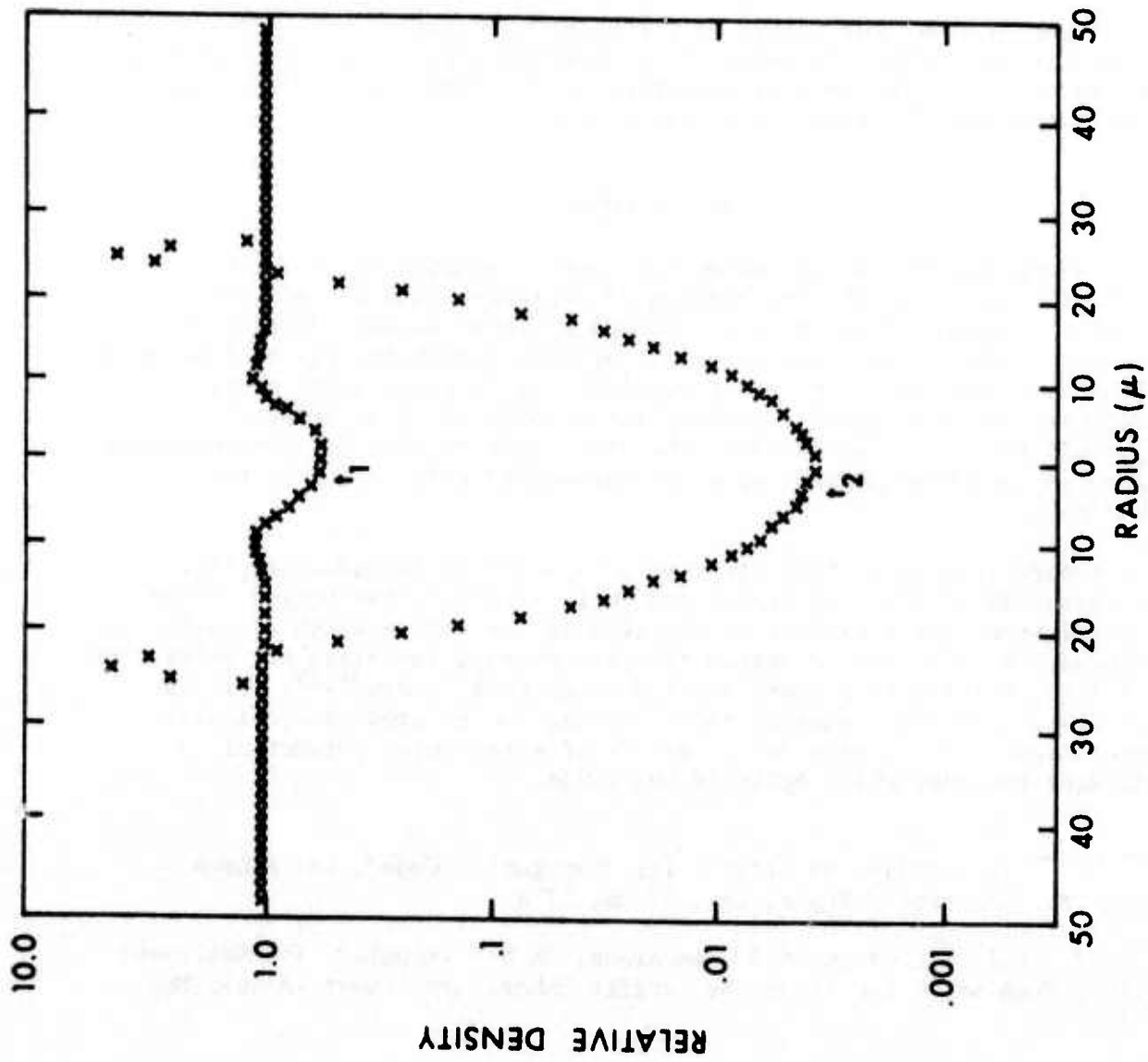


Figure 6. Same type of plot as Figure 5 except that the radial pulse shape is Gaussian with a full width at half maximum of 10μ .

REFERENCES

1. T. F. Stratton, "A High Energy, Short Pulse CO₂ Laser System", VIII International Quantum Electronics Conference, San Francisco, CA, June, 1974, Abstract B.2.
2. A. Crocker, H. M. Lamberton, E. W. Parcell and H. C. Probyn, "500 J CO₂ Electron Beam Laser Controlled by a Glow Discharge Electron Gun", VIII International Quantum Electronics Conference, San Francisco, CA, June, 1974, Abstract B.4.
3. A. Wayne Johnson and J. B. Gerardo, "The Vacuum-Ultra-Violet Xenon Laser", VIII International Quantum Electronics Conference, San Francisco, CA, June, 1974, Abstract M.2.
4. M. A. Duguay and P. M. Rentzepis, "Some Approaches to Vacuum UV and X-Ray Lasers", Appl. Phys. Letters, Vol. 10, 350 (1967).
5. R. C. Elton, R. W. Waynant, R. A. Andrews, and M. H. Reilly, "X-Ray and Vacuum-UV Lasers", NRL Report 7412, May, 1972.
6. P. J. Mallozzi, et al., "X-Ray Emission from Laser-Generated Plasmas", ARPA Technical Report 1723, Jan., 1972.
7. M. O. Scully, W. H. Louisell, and W. B. McKnight, "A Soft X-Ray Laser Utilizing Charge Exchange", VIII International Quantum Electronics Conference, San Francisco, CA, June, 1974, Abstract M.9.
8. R. A. McCorkle, and J. M. Joyce, "Threshold Conditions for Amplified Spontaneous Emission of X Radiation", Phys. Rev. A, Vol. 10, 1974, p. A903.
9. J. G. Kepros, E. M. Eyring, F. W. Cagle, Jr., "Experimental Evidence of an X-Ray Laser", Proc. Nat. Acad. Sci. USA, Vol. 69, 1972, p. 1744.
10. R. A. Andrews, "X-Ray Lasers-Current Thinking", NRL Memorandum Report 2677, October, 1973.
11. R. C. Elton, "Analysis of X-Ray Laser Approaches: 2. Quasistationary Inversion on K α -Innershell Transitions", NRL Memorandum Report 2906, October, 1974.
12. D. W. Missavage and S. T. Manson, "Photoionization of Positive Ions of Atomic Oxygen", Phys. Letters, Vol. 38A, 1972, p. 85.
13. M. D. Torrey, N. A. Zessoules, and W. D. Lanning, "Numerical Simulation Techniques for Nonequilibrium Effects of High-Altitude Nuclear Detonations", Technical Operations Research, Report No. TO-B 66-29, May, 1966.

14. F. Biggs and R. Lighthill, "Analytical Approximations for X-Ray Cross Sections II", Sandia Laboratories, Report No. SC-RR-71 0507, December, 1971.
15. A. H. Compton and S. K. Allison, X-Rays in Theory and Experiment, Van Nostrand, Princeton, N.J., 1935, pp. 564-582.
16. W. Bambynik, B. Craseman, R. W. Fink, H. U. Freund, H. Mark, C. D. Swift, R. E. Price, and P. V. Rao, "X-Ray Fluorescence Yields, Auger, and Coster-Kronig Transition Probabilities", Rev. Mod. Phys., Vol. 44, 1972, p. 716.
17. E. U. Condon, "X-Rays", in Handbook of Physics edited by E. U. Condon and H. Odishaw, McGraw-Hill, New York, 1958, p. 7-124.
18. R. D. Evans, The Atomic Nucleus, McGraw-Hill, New York, 1955, p. 582.
19. Ibid, p. 580.
20. Kai Siegbahn, Alpha-, Beta-, and Gamma-Ray Spectroscopy, North-Holland, Amsterdam, 1966, p. 26.
21. P. I. Richards, "Summary Report on Investigation of Radiation and Chemical Calculations", Technical Operations Research, Report No. TO-B 62-24 May, 1962.
22. R. D. Evans, op. cit., p. 684.
23. Ibid, p. 688.
24. P. I. Richards, "The Tech/Ops Two-Dimensional Time-Dependent Hydrodynamics Code", Technical Operations Research, Report No. TO-B 62-22, April, 1962.
25. T. A. Carlson, C. W. Nestor, Jr., T. C. Tucker, and F. B. Malik, "Calculation of Electron Shake-off for Elements from $Z = 2$ to 92 with the use of Self-Consistent-Field Wave Functions", Phys. Rev., Vol. 169, 1968, p. 27.
26. T. A. Carlson and M. O. Krause, "Experimental Evidence for Double Electron Emission in an Auger Process", Phys. Rev. Letters, Vol. 14, 1965, p. 390.
27. M. O. Krause, M. L. Vestal, W. H. Johnston, and T. A. Carlson, "Readjustment of the Neon Atom Ionized in the K Shell by X-Rays", Phys. Rev. A, Vol. 133, 1964, p. A385.

28. T. A. Carlson and M. O. Krause, "Electron Shake-off Resulting from K-Shell Ionization in Neon Measured as a Function of Photoelectron Velocity", Phys. Rev. A, Vol. 140, 1965, p. A1057.
29. Howard D. Cohen, Donald E. Parks, and Albert G. Petschek, "A Study of Equations of State/Opaicity of Ionized Gases", SYSTEMS, SCIENCE and SOFTWARE, Report No. DASA 2597-1, April, 1971.
30. J. C. Stewart and K. D. Pyatt, "Lowering of Ionization Potentials in Plasmas", Ap. J., Vol. 144, 1966, p. 1203.
31. D. E. Parks, G. Lame, J. C. Stewart, and S. Peyton, "Optical Constants of Uranium Plasma", NASA Report No. CR-72348[GA8244], 1967.
32. Lyman Spitzer, Jr., Physics of Fully Ionized Gases, Interscience, 1962, p. 150.
33. D. R. Bates, "Electron Recombination in Helium", Phys. Rev., Vol. 77, 1950, p. 718.
34. D. R. Bates, "Dissociative Recombination", Phys. Rev., Vol. 78, 1950, p. 492.
35. E. C. G. Stueckelberg and P. M. Morse, "Computations of the Effective Cross Section for the Recombination of Electrons With Hydrogen Ions", Phys. Rev., Vol. 36, 1930, p. 16.
36. B. R. Suydam, "A Laser Pulse Propagation Code", Los Alamos Scientific Laboratory Report LA-5607-MS, 1974.
37. C. J. Elliot and D. B. Henderson, "A New Technique for Nonlinear Optical Problems", Los Alamos Scientific Laboratory Report LA-5639-MS, 1974.

DISTRIBUTION LIST

<u>No. of Copies</u>	<u>Organization</u>	<u>No. of Copies</u>	<u>Organization</u>
2	Commander Defense Documentation Center ATTN: DDC-TCA Cameron Station Alexandria, VA 22314	1	Director US Army Air Mobility Research and Development Laboratory Ames Research Center Moffett Field, CA 94035
1	Director Defense Advanced Research Projects Agency ATTN: Dr. Edward T. Gerry 1400 Wilson Boulevard Arlington, VA 22209	1	Commander US Army Electronics Command ATTN: AMSEL-RD Fort Monmouth, NJ 07703
2	Commander US Army Materiel Command ATTN: AMCDMA Mr. N. Klein Mr. J. Bender 5001 Eisenhower Avenue Alexandria, VA 22333	1	Commander US Army Missile Command ATTN: AMSMI-R Redstone Arsenal, AL 35809
1	Commander US Army Materiel Command ATTN: AMCRD, BG H.A. Griffith 5001 Eisenhower Avenue Alexandria, VA 22333	2	Commander US Army Missile Command ATTN: AMSMI-RV Dr. W. B. McKnight Dr. John Hammond Redstone Arsenal, AL 35809
1	Commander US Army Materiel Command ATTN: AMCRD-T, Dr. B. Zarwyn 5001 Eisenhower Avenue Alexandria, VA 22333	1	Commander US Army Tank Automotive Command ATTN: AMSTA-RHFL Warren, MI 48090
1	Commander US Army Materiel Command ATTN: AMCRD-WN, J. Corrigan 5001 Eisenhower Avenue Alexandria, VA 22333	2	Commander US Army Mobility Equipment Research & Development Center ATTN: Tech Docu Cen, Bldg. 315 AMSME-RZT Fort Belvoir, VA 22060
1	Commander US Army Aviation Systems Command ATTN: AMSAV-E 12th and Spruce Streets St. Louis, MO 63166	1	Commander US Army Armament Command Rock Island, IL 61202
		2	Commander US Army Harry Diamond Labs ATTN: AMXDO-TI AMXDO-NP, Dr. M. Cohen 2800 Powder Mill Road Adelphi, MD 20783

DISTRIBUTION LIST

<u>No. of Copies</u>	<u>Organization</u>	<u>No. of Copies</u>	<u>Organization</u>
2	Commander US Army Harry Diamond Labs ATTN: AMXDO-TD Dr. H. Sommer Dr. W. Carter 2800 Powder Mill Road Adelphi, MD 20783	2	Commander US Naval Research Laboratory ATTN: Dr. R. C. Elton R. H. Andrews Washington, DC 20375
1	HQDA (DAMA-ZC, Dr. Marvin E. Lasser) Washington, DC 20310	1	Polytechnic Institute Nuclear Science Department at Rensselaer ATTN: Prof. George C. Baldwin Troy, NY 12181
1	HQDA (DAMA-ARS-P, Dr. R. B. Watson, Physical & Eng. Sciences Office) Washington, DC 20310	1	University of Southern California Department of Physics ATTN: Dr. William B. Louisell Los Angeles, CA 90007
3	Director US Army Research Office ATTN: RDRD-RT-E, Dr. Mace Dr. Cifton Dr. Lontz Box CM, Duke Station Durham, NC 27706		<u>Aberdeen Proving Ground</u> Marine Corps Ln Ofc Dir, USAMSAA Cmdt, USAOC&S ATTN: ATSL-CTD-MS-R Dr. Thomas J. Welch
2	Director US Army Ballistic Missile Defense Program Office ATTN: DACS-BMM, Mr. A. Gold Mr. Martin Zlotnick 1300 Wilson Boulevard Arlington, VA 22209		